

Superconducting coherence peak in the electronic excitations of a single layer cuprate superconductor $\text{Bi}_2\text{Sr}_{1.6}\text{La}_{0.4}\text{CuO}_{6+\delta}$

J. Wei,¹ Y. Zhang,¹ H. W. Ou,¹ B. P. Xie,¹ D. W. Shen,¹ J. F. Zhao,¹ L. X. Yang,¹ M. Arita,²
K. Shimada,² H. Namatame,² M. Taniguchi,² Y. Yoshida,³ H. Eisaki,³ and D. L. Feng^{1,*}

¹*Department of Physics, Surface Physics Laboratory (National Key Laboratory) and Advanced Materials Laboratory, Fudan University, Shanghai 200433, P. R. China*

²*Hiroshima Synchrotron Radiation Center and Graduate School of Science, Hiroshima University, Hiroshima 739-8526, Japan*

³*National Institute of Advanced Industrial Science and Technology (AIST), Tsukuba, Ibaraki, 3058568, Japan*
(Dated: February 9, 2022)

Angle resolved photoemission spectroscopy study is reported on a high quality optimally doped $\text{Bi}_2\text{Sr}_{1.6}\text{La}_{0.4}\text{CuO}_{6+\delta}$ high- T_c superconductor. In the antinodal region with maximal d -wave gap, the symbolic superconducting coherence peak, which has been widely observed in multi- CuO_2 -layer cuprate superconductors, is unambiguously observed in a single layer system. The associated peak-dip separation is just about 19 meV, which is much smaller than its counterparts in multi-layered compounds, but correlates with the energy scales of spin excitations in single layer cuprates.

In search of the mechanism of high temperature superconductivity, one central issue is whether there are certain bosons that play the critical mediating role of phonons in conventional BCS superconductor. Specifically, if there were such bosons, what would they be? So far, signatures of electron-boson interactions have been identified in single particle excitations measured by angle resolved photoemission spectroscopy (ARPES). For example, in the so-called nodal region, where the d -wave superconducting gap diminishes, a characteristic kink [1, 2] was discovered in the dispersion of various cuprate superconductors. However, the nature of the corresponding boson, particularly whether it is due to lattice or spin excitations, was intensively debated.

For multi- CuO_2 -layer cuprate superconductors, such as $\text{Bi}_2\text{Sr}_2\text{CaCu}_2\text{O}_{8+\delta}$ (Bi2212), $\text{Bi}_2\text{Sr}_2\text{Ca}_2\text{Cu}_3\text{O}_{10+\delta}$ (Bi2223) and $\text{YBa}_2\text{Cu}_3\text{O}_{7-\delta}$ (YBCO) [3, 4, 5, 6, 7], a sharp peak emerges out of the normal state broad spectrum when temperature is lowered below the superconducting transition temperature (T_c), forming a so-called “peak-dip-hump” (PDH) structure (see Fig. 4c for illustration) in the antinodal region, where d -wave superconducting gap is at its maximum. This sharp peak, also termed as superconducting coherence peak (SCP), contains rich information about superconductivity. Its position reflects the maximal pairing strength, while its intensity grows with decreasing temperature, illustrating the gain of coherence through the development of superconducting condensate or superfluid [4, 8, 9]. The PDH structure has been regarded as an evidence for interactions with a bosonic mode [10, 11, 12, 13, 14, 15, 16, 17, 18]. However, since this mode energy (~ 35 meV) coincides with the energy of certain oxygen phonon and spin excitations near (π, π) , scenarios based on both kinds of bosons have been put forward.

In spite of its importance, an unambiguous observation of SCP or two-component spectrum in the antinodal region of single layer compounds is so far lacking

[6, 19, 20, 21, 22]. In this letter, we report the discovery of the antinodal SCP in an optimally doped single layer $\text{Bi}_2\text{Sr}_2\text{CuO}_{6+\delta}$ (Bi2201). We found the peak-dip distance to be about 19 meV, suggesting the possibility of a bosonic mode in Bi2201 with a much lower energy than that in Bi2212. This low energy mode seems to correlate with the superconducting gap and the energy scale of spin excitations observed in various single layer compounds.

$\text{Bi}_2\text{Sr}_{1.6}\text{La}_{0.4}\text{CuO}_{6+\delta}$ (La-Bi2201) single crystals were grown with the floating zone technique. Its superior quality is manifested through the very high T_c (34K) in its class, and a remarkable zero residual resistivity [23, 24], which is critical for revealing the intrinsic properties of high- T_c superconductors. The sample is optimally doped, as verified by the linear temperature dependence of resistivity, and detailed annealing studies. The ARPES experiments were conducted with 22.5 eV photons and a Scienta-R4000 electron analyzer at beamline 9 of Hiroshima synchrotron radiation center. The energy resolution was 7 meV. The samples were cleaved in ultra-high vacuum ($\sim 5 \times 10^{-11}$ mbar), and measured within 10 hours. The experiments on Bi2212 and Bi2223 were conducted with 22.7 eV photons and a Scienta-200 electron analyzer at beamline 5-4 of Stanford synchrotron radiation laboratory (SSRL). The energy resolutions was 10 meV. Angular resolution was 0.3° for all experiments.

Photoemission data in the superconducting state of La-Bi2201 are shown in Fig. 1 along eight cuts across the Fermi surface. The data were taken in the Γ -Y quadrant of the Brillouin zone, so that superstructure band is well separated from the main band. Sharp quasiparticle shows clear dispersion in the nodal region [Fig. 1(a1,b1)]. The departure from a linear dispersion, or a kink, in the energy range of 40~70 meV could be observed in the first three cuts [Fig. 1(a1-a3)]. The kink diminishes further away from the nodal region [Fig. 1(a4)], while starting from cut #5 in the antinodal region, a feature near

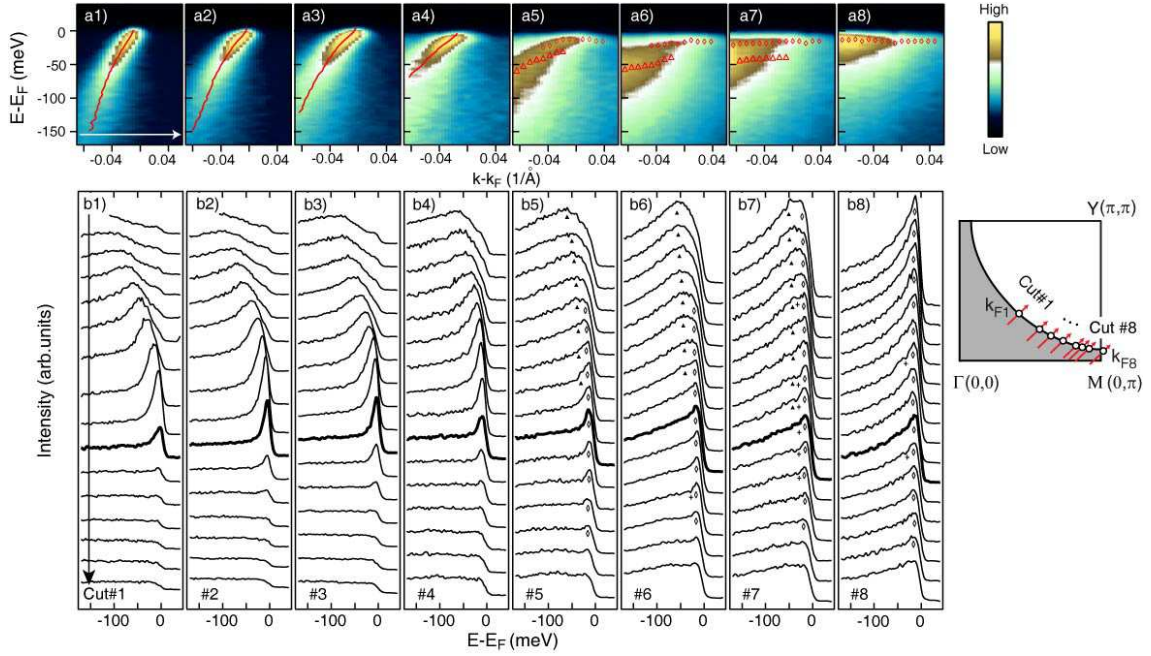


FIG. 1: (Color online) Photoemission data of La-Bi2201. (a1-a8) photoemission intensity map along cut #1-#8 across the Fermi surface, as illustrated by arrows on the right. The data were taken at 20K in the superconducting state. Thick lines in a1-a4 are the dispersions fitted from momentum distribute curves. (b1-b8) display the corresponding spectra in panel a1-a8. The spectra at various Fermi crossings ($k_{Fi}, i = 1, 2, \dots, 8$, marked by black dots) are in thick curves. The “peak”, “dip” and “hump” structures are represented by diamonds, crosses and triangles respectively.

the Fermi energy (E_F) gradually becomes quite prominent as indicated by the diamonds in Fig. 1(a5-a8, b5-b8). Along the cuts #5-#7, there is also a broad feature at higher binding energy as labeled by the triangles. Though weak, the appearance of such two-component structure over a broad momentum area clearly proves its robustness against the experimental uncertainties. Eventually, a weak PDH feature is observed in some spectra. In the vicinity of $(\pi, 0)$ [Fig. 1(a8, b8)], the overall lineshape becomes sharper and closer to the E_F , so the two components become indistinguishable. We emphasize the sharp peak in the antinodal region is so delicate that it disappears further away from the Fermi surface, where the scattering becomes stronger. Therefore, we attribute the discovery of the two-component lineshape to the minimized disorder effects in La-Bi2201 [23, 24]. We also note that the evolution from the nodal kink to the antinodal PDH in Bi2201 is quite different from that in Bi2212. For Bi2212, the kink becomes increasingly pronounced away from the node, and gradually evolves into the PDH in the antinodal region [2, 14]. This highlights the subtle differences between single layer and multi-layer cuprates.

The two-component lineshape in the antinodal region alludes to the existence of SCP in La-Bi2201. To further evidence this, the temperature dependences along the cut #1 and #6 are compared in Fig. 2. While the nodal kink structure is temperature independent [Fig. 2(a1-a3)], a sharp peak along cut #6 gradually emerges out of the

normal state broad spectra with decreasing temperature [Fig. 2(b1-b3)], which is more discernible in the energy distribution curves (EDCs) shown in Fig. 2(c1-c3). As further illustrated in Fig. 3(a-b) for two momenta in the antinodal region, the sharp peak appears only below T_c , and saturates at low temperatures, just like the temperature dependence of a SCP [4]. We note that the formation of the dip feature is particularly distinct here as well. Moreover, to show this sharp peak is not simply due to thermal effect, the normal state spectrum at k_{F7} is divided by the resolution convoluted Fermi function of 35K and then multiplied by that of 10K, before it is compared with the corresponding 10K spectrum in Fig. 3c. The difference is very clear, and sharp peak thus cannot be reproduced from thermal sharpening. For comparison, following the same procedure, the nodal spectra taken at both below and above T_c overlap with each other (Fig. 3d). Therefore, both the temperature and momentum dependence evidence that the sharp peak in the antinodal region is the SCP as observed in multi-layered cuprates before. It unambiguously rules out scenarios that suggest PDH being caused by bilayer band splitting.

The properties of the SCP provide important information about superconductivity. Fig. 4(a) shows the associated PDH structures for three momenta near $(\pi, 0)$. Through a phenomenological fitting [4], one could precisely determine the peak position and the separation between the peak and dip, which is about 19 meV at

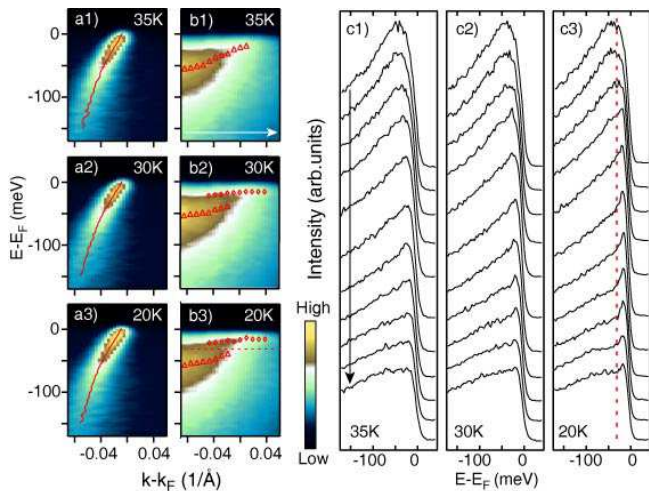


FIG. 2: (Color online) Temperature dependence of La-Bi2201 ($T_c=34K$) photoemission data along (a1-a3) the nodal direction, and (b1-b3) along cut #6. (c1-c3) The EDCs of data in panel b1-b3 respectively. The red dashed line indicates the break between the peaks (diamonds) and humps (triangles).

all three momenta. Similarly, the peak dip structure in Bi2212 ($T_c = 90K$) also possesses a constant separation of 33 meV at these momenta (Fig. 4b), and $(\pi, 0)$ (Fig. 4c). On the other hand, the peak-dip separations are about 34 meV for Bi2223 ($T_c = 108K$) and the recently synthesized Bi2212 ($T_c = 96K$). If one would follow the same analyses as in many previous ARPES studies that the peak-dip separation corresponds to the energy of a bosonic mode [10, 11, 12, 13, 14, 15, 16, 17], our Bi2201 data would suggest a bosonic mode of about 19 meV that interacts with the electrons in the antinodal regions. Such a low energy mode could not be one of the oxygen-related phonons, which are all above 35 meV as shown by Raman scattering experiments[25]. In the phonon picture, one then needs different phonons to explain the PDH in Bi2212 and Bi2201. The oxygen B_{1g} -phonon, which was argued to be responsible for the PDH in Bi2212[13, 14], is forbidden by symmetry in Bi2201. Phonons of heavy ions are needed to explain the low energy feature in Bi2201[25]. On the other hand, the peak-dip separations have an intriguing correlation with the energy scale of spin excitations near (π, π) measured by inelastic neutron scattering on YBCO [26], Bi2212 [27, 28], $\text{Pr}_{0.88}\text{LaCe}_{0.12}\text{CuO}_{4-\delta}$ (PLCCO) [29], and $\text{La}_{2-x}\text{Sr}_x\text{CuO}_4$ (LSCO) [30] as a function of T_c (Fig. 4d). Although inelastic neutron scattering measurement of Bi2201 is currently lacking, the Bi2201 peak-dip separation falls in the dashed line representing the energy scale of the spin excitations. Moreover, the temperature dependence of the dip structure also resembles that of the neutron resonance mode [8, 17, 28] which emerges only below T_c and develops into a sharp collective spin excitation at very low temperatures. The weaker dip structure

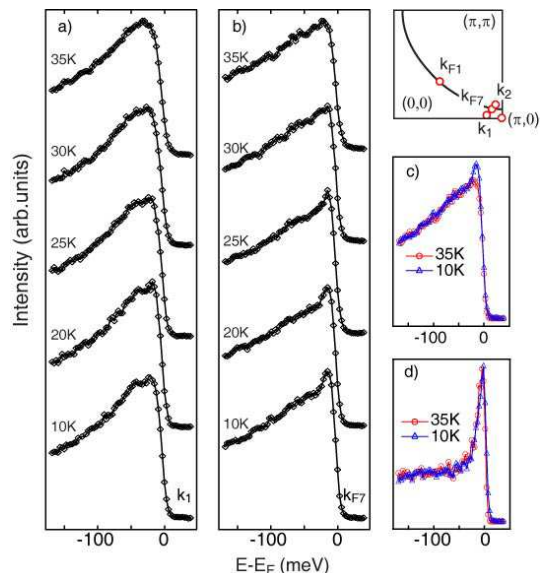


FIG. 3: (Color online) Detailed temperature dependence of photoemission data at (a) k_1 and (b) k_{F7} respectively, in the vicinity of $(\pi, 0)$ as indicated in the inset. (c) and (d) compare the spectra below and above T_c at k_{F7} and k_{F1} respectively, after removing the temperature broadening effects (see text for details).

in Bi2201 is consistent with the weaker intensity of the spin excitations observed in low- T_c systems [29, 30]. Furthermore, as shown in Fig. 4e, the Bi2201 SCP position, i.e., the superconducting gap amplitude, together with those of other optimally doped cuprates, correlates with T_c , and the energy scale of the spin excitations. This resembles the correspondence among the Debye frequency of phonon, the superconducting gap, and T_c in the BCS theory.

Recent analysis of the Bi2212 scanning tunneling microscopy (STM) data [18] suggested that the mode energy could be the separation between the peak and the higher binding energy edge of the dip in the measured density of state, due to the complication of the scattering matrix element and detailed energy and momentum distribution of the states. In this regard, further theoretical analysis is necessary to conclude if the peak-dip separation in ARPES antinodal spectrum exactly corresponds to the bosonic mode energy. Literally following the STM analysis on antinodal spectra, we obtained a slightly larger mode energy of about 23 meV. From a different perspective, the two-component lineshapes, particularly the breaks in dispersions between the peak and hump features [e.g., the red dashed lines in Fig. 2(b3) and (c3)], are also possible signs of interactions between electrons and bosons. The distance between the peak position at the Fermi momentum and the top of the hump feature gives an upper limit of 25 meV for the mode. These all robustly and self-consistently indicate a low

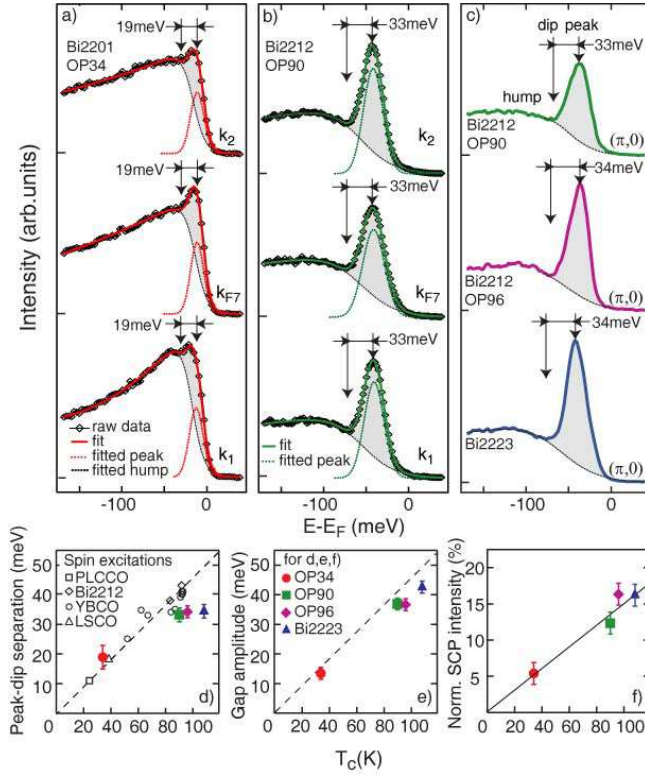


FIG. 4: (Color online) SCP near $(\pi,0)$ for (a) optimally doped single layer $\text{Bi}_2\text{Sr}_{1.6}\text{La}_{0.4}\text{CuO}_{6+\delta}$ ($T_c=34\text{K}$, OP34) and (b) bilayer $\text{Bi}_{2.1}\text{Sr}_{1.9}\text{CaCu}_2\text{O}_{8+\delta}$ ($T_c=90\text{K}$, OP90) at three momenta (k_1 , k_2 , and k_{F7} are illustrated in the inset of Fig. 3). (c) Spectra at $(\pi,0)$ for OP90, $\text{Bi}_2\text{Sr}_2\text{Ca}_{0.92}\text{Y}_{0.08}\text{Cu}_2\text{O}_{8+\delta}$ ($T_c=96\text{K}$, OP96) and Bi2223 ($T_c=108\text{K}$). Peak and dip positions are illustrated by the arrows. (d) The peak-dip separation vs. T_c for single, bi- and tri-layer bismuth cuprates near optimal doping. The energies of spin excitations near (π, π) for YBCO [26], Bi2212 [27, 28], PLCCO [29] and LSCO [30] are plotted for comparison. (e) The superconducting gap amplitude, and (f) the intensity of SCP (shaded region in a,c) normalized by the total spectral weight over $[E_F-0.5\text{eV}, E_F+0.1\text{eV}]$ as a function of T_c . The SCP is determined from a phenomenological fitting (dashed curves) [4, 6]. The dashed lines in (d-e) are a fit to the spin excitation energy. The solid line in (f) is a guide to the eye.

energy mode active in the antinodal region.

Besides the interpretation of electron-boson interactions for PDH, our data seem also fit in an alternative scenario, where the SCP was considered as the emergence of a coherent quasiparticle out of the broad incoherent background upon superfluid formation[4]. The SCP intensity was found to correlate almost linearly with the superfluid density for Bi2212, as a signature for High- T_c superconductor being a doped Mott insulator[4, 8, 31]. The new La-Bi2201 data fits in a linear relation between relative intensity of SCP and the optimal T_c (Fig. 4f). Moreover, for the more stoichiometric $\text{Bi}_2\text{Sr}_2\text{Ca}_{0.92}\text{Y}_{0.08}\text{Cu}_2\text{O}_{8+\delta}$ (OP96), whose T_c is enhanced to 96K from the usual optimal T_c of 90K [23, 24], its SCP intensity is en-

hanced, while its gap is similar to that of OP90. Meanwhile, OP96 and Bi2223 have similar SCP intensities, but Bi2223 has a larger gap. These illustrate that improving either the gap size or phase coherence would enhance T_c [6, 32], and the low T_c of Bi2201 system is probably due to both its small gap size and low superfluid density[24, 31].

To summarize, we have discovered the SCP in the antinodal region of the single layer La-Bi2201. In particular, we show that its 19 meV peak-dip separation intriguingly correlates with the energy scale of spin fluctuations. Our data provides a critical piece to the global picture, which would help to eventually resolve controversial issues and uncover the “glue” of high- T_c superconductivity.

We gratefully acknowledge the helpful discussions with Dr. W. S. Lee, D. H. Lu, Profs. Z.-X. Shen, D. H. Lee, T. P. Devereaux and C. Y. Kim. This work was supported by NSFC, MOST (973 project No.2006CB921300 and No.2006CB601002), and STCSM of China. SSRL is operated by the DOE Office of Basic Energy Science Divisions of Chemical Sciences and Material Sciences.

* Electronic address: dlifeng@fudan.edu.cn

- [1] A. Damascelli, Z. Hussain, Z. X. Shen, *Rev. Mod. Phys.* **75**, 473 (2003).
- [2] T. Cuk *et al*, *Phys. Stat. Sol. (b)* **242**, 11 (2005).
- [3] D. S. Dessau *et al*, *Phys. Rev. Lett.* **66**, 2160 (1991).
- [4] D. L. Feng *et al*, *Science* **289**, 277 (2000), which also has the details for the phenomenological fitting procedures exploited in Fig.4.
- [5] D. H. Lu *et al*, *Phys. Rev. Lett.* **86**, 4370 (2001).
- [6] D. L. Feng *et al*, *Phys. Rev. Lett.* **88**, 107001 (2002).
- [7] H. Matsui *et al*, *Phys. Rev. Lett.* **90**, 217002 (2003).
- [8] R. H. He *et al*, *Phys. Rev. B* **69**, 220502(R) (2004).
- [9] H. Ding *et al*, *Phys. Rev. Lett.* **87**, 227001 (2001).
- [10] J. C. Campuzano *et al*, *Phys. Rev. Lett.* **83**, 3709 (1999).
- [11] M. R. Norman, H. Ding, *Phys. Rev. B* **57**, 11089 (1998).
- [12] Z. X. Shen, J. R. Schrieffer, *Phys. Rev. Lett.* **78**, 1771 (1997).
- [13] T. P. Devereaux, T. Cuk, Z. X. Shen, N. Nagaosa, *Phys. Rev. Lett.* **93**, 117004 (2004).
- [14] T. Cuk *et al*, *Phys. Rev. Lett.* **93**, 117003 (2004).
- [15] Ar. Abanov, A. Chubukov, *Phys. Rev. Lett.* **83**, 1652 (1999).
- [16] M. Eschrig, M. R. Norman, *Phys. Rev. Lett.* **85**, 3261 (2000), *ibid.* **89**, 277005 (2002).
- [17] J. F. Zasadzinski *et al*, *Phys. Rev. Lett.* **87**, 067005 (2001).
- [18] J. Lee *et al*, *Nature* **442**, 546 (2006).
- [19] T. Kondo *et al*, *Phys. Rev. Lett.* **98**, 267004 (2007).
- [20] K. Terashima *et al*, *Phys. Rev. Lett.* **99**, 017003 (2007).
- [21] M. Plate *et al*, *Phys. Rev. Lett.* **95**, 077001 (2005).
- [22] W. S. Lee *et al*, *Arxiv:cond-mat/0606347*.
- [23] K. Fujita *et al*, *Phys. Rev. Lett.* **95**, 097006 (2005).
- [24] H. Eisaki *et al*, *Phys. Rev. B* **69**, 064512 (2004).
- [25] R. Liu *et al*, *Phys. Rev. B* **45**, 7392 (1992).
- [26] J. Bok *et al*, Eds. (Plenum, New York, 1998), p. 349-371. *Arxiv:cond-mat/9901333*, and references there in.
- [27] H. F. Fong *et al*, *Nature* **398**, 588 (1999).

- [28] H. He. *et al*, Phys. Rev. Lett. **86**, 1610 (2001).
- [29] S. D. Wilson *et al*, Nature **442**, 59 (2007).
- [30] B. Vignolle *et al*, Nature Physics **3**, 163 (2007).
- [31] Y. J. Uemura *et al*, Phys. Rev. Lett. **62**, 2317 (1989);
Physica C **282**, 194 (1997).
- [32] V. J. Emery, S. A. Kivelson, Nature(London) **374**, 434 (1995).